RAPID COMMUNICATIONS

PHYSICAL REVIEW B VOLUME 43, NUMBER 11 15 APRIL 1991-I

Long-wavelength infrared spectroscopy of an asymmetrically structured $Ga_{0.6}Al_{0.4}As/GaAs$ superlattice

Shmuel I. Borenstain and Ilan Gravé
Department of Applied Physics, California Institute of Technology, Pasadena, California 91125

Anders Larsson and Daniel H. Rich
Jet Propulsion Laboratory, 4800 Oak Grove Drive, Pasadena, California 91109

Bjorn Jonsson, Ingmar Andersson, Johan Westin, and Thorwald Andersson
Chalmers University of Technology, S-412 96 Goteborg, Sweden
(Received 8 November 1990; revised manuscript received 1 February 1991)

A long-wavelength infrared (LWIR) spectroscopic study of a doped multiple-quantum-well (MQW) structure, where each quantum well is clad by asymmetrically structured superlattices, is reported. The measured absorption and photocurrent spectra differ markedly from those of a MQW LWIR detector with conventional flat barriers. Different electron subband states are introduced, and the transition $e1$-$e3$, which in a flat-barrier MQW is normally forbidden, becomes the dominant transition; thus bringing about an extremely broad photoresponse band ($\Delta\lambda/\lambda \approx 0.6$), centered at 5 μm. This system also exhibits direct evidence of photon-assisted resonant tunneling. It is manifested by a distinct peak and negative differential photoconductance in the photocurrent-vs-bias-voltage characteristics when the structure is exposed to a CO_2 9.5-μm laser line. All these effects are explained by the dependence of the electronic eigenstate spectrum on the electric field, calculated by solving the Schrödinger equation using the transfer-matrix method.

Long-wavelength infrared (LWIR) opto-electrical studies of intersubband and subband-to-continuum transitions in multiple-quantum-well (MQW) structures[1-20] have recently been the focus of intense research because of the variety of applications which are considered possible for this system such as LWIR detectors,[7] highly efficient second-harmonic generators,[8] and LWIR lasers.[9-11] In this class of band-gap-engineered devices, the properties of asymmetrically built MQW's have been investigated primarily for the purpose of inducing nonlinear effects for second-harmonic generation. With regard to LWIR MQW detectors, it has been shown recently that by introducing asymmetry to a quantum well (QW), forbidden transitions become allowed, and also a large infrared (IR) Stark shift is induced which makes tunable detectors possible. An obvious way to achieve symmetry breaking in a MQW is by applying an electric-field across the structure. However, in order to observe nonlinear effects, the applied electric field must be extremely large and excessive background currents are generated. Recently, various symmetry-breaking techniques have been implemented, e.g., stepped QW,[12] asymmetrically doped QW with the extreme of δ-doped donor layers located next to the barrier,[13] and asymmetrically sloped barriers created by gradual variation of the Al concentration in the $Al_xGa_{1-x}As$ barrier.[14] In this work, we have investigated the properties of a MQW where the doped QW's are clad by variably spaced superlattices such that the symmetry about the center of the QW's is broken. Our main result springs from allowing forbidden transitions and suggests that $GaAs/Ga_{1-x}Al_xAs$-based MQW detectors can cover the 3–6-μm atmospheric window, in contradiction to earlier predictions.[4]

The original motivation for this work is an examination of the filtering effect believed to occur in such structures,[15] termed variably spaced superlattice energy filters (VSSEF). By exciting electrons into highly conductive energy channels in the VSSEF barriers, a "monochromatic" electron beam may be created. This can be used for the creation of population inversion within subbands, a necessary condition for LWIR laser operation.[16] Other structures which utilize photon assisted resonant tunneling as electronic energy filters for LWIR detectors, have been investigated.[3,5] In this paper, we report on a direct evidence for photon assisted resonant tunneling, and on a spectroscopic study performed on the structure. The analysis of the data, based on solving the Schrödinger equation using the transfer-matrix technique, provides a comprehensive picture of the electro-optic properties of this structure.

The conduction-band diagram of the device is shown in Fig. 1. The structure was grown by molecular-beam epitaxy on an n-doped GaAs substrate, and consists of 30 QW's separated by VSSEF barriers. The entire MQW is clad by n-doped GaAs contact layers. The center of each of the 28 monolayer thick QW's was doped with Si donors, leaving 10 Å undoped next to the adjacent barriers. From Hall measurements we find an average carrier density of 1.5×10^{18} cm^{-3} in the doped QW's. The measured carrier concentration is indicative of a Fermi energy of -44 meV from the ground state of the doped QW at 0 K. Detector elements were formed by etching 90-μm diam mesas, 2 μm high. The edge of the detector chip was polished at 45° to allow the light to enter the structure with some polarization parallel to the growth direction, as is required for LWIR MQW detectors.[4] The

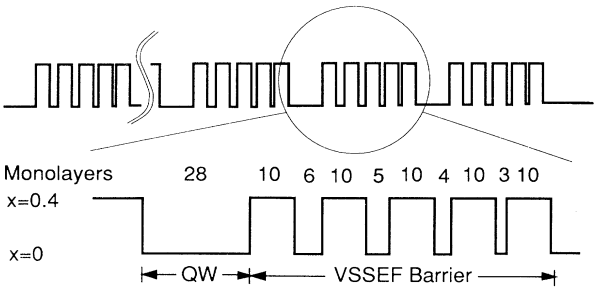

FIG. 1. Conduction-band diagram of the asymmetrically structured MQW structure.

detector chip was cemented to a copper block, and the whole assembly was mounted in a cryostat for LWIR photocurrent characterization. The dark current of the detector at 4 V ranged from 50 μA at 20 K to $\sim$1 mA at 80 K, which is too high for the detector to be practical. The spectra depicted in Fig. 2 were measured using a Fourier spectrometer. The photoresponse spectrum was normalized to the flat response of a pyroelectric detector. The absorption spectrum was measured on a planar waveguide, polished at 45° at both ends of the slab.[1] It was taken using an IR polarizer, and the absorbance value was evaluated as $\log_{10}(T_-/T_+)$, where T_- and T_+ are the transmission taken with the polarizer aligned parallel and normal to the growth direction, respectively. This technique allows one to measure a polarized absorption band embedded in a very large background, which in our case is mainly due to free-carrier absorption in the substrate. The Si impurity band is not expected to introduce any additional components in the absorption spectra. At room temperature (RT) most of the donors are ionized as determined from Fermi statistics, and thus the RT absorption spectrum [see Fig. 2(a)] is dominated by the excitation of

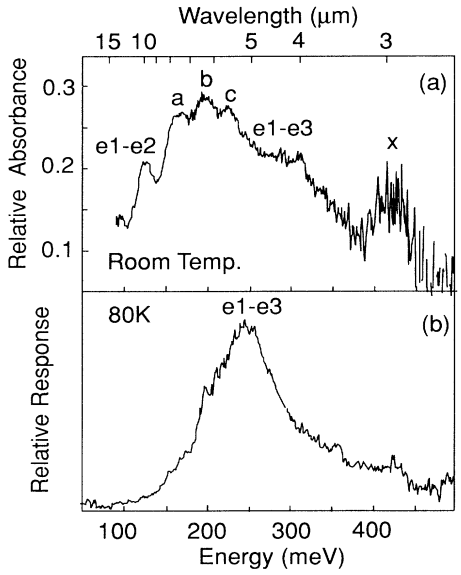

FIG. 2. (a) Measured absorbance vs photon energy taken with a planar waveguide slab. (b) Measured photocurrent response at a bias of 4 V.

free electrons. Also, from previous intersubband absorption measurements of heavily doped MQW's with a single excited level, a single absorption peak was measured even at low temperatures.[1,6,18,19]

Let us discuss the origin of the peaks observed in Fig. 2. We consider first transitions to states that exist also in a flat-barrier symmetrical QW (FBSQW). The first of these is the allowed transitions, marked $e1$-$e2$ in Fig. 2(a). The state $e3$ exists also in a FBSQW, but the transition $e1$-$e3$ is forbidden by parity; it becomes allowed here due to symmetry breaking.[12–14] This transition is indeed dominant in the photocurrent spectrum of Fig. 2(b). However, it is difficult to unambiguously identify it in the absorption spectrum of Fig. 2(a). The temperature difference between the two spectra cannot contribute to a subband energy shift of more than 4 meV (Ref. 6) or to a substantial broadening.[6] Also, our photoresponse data shows that this transition is relatively insensitive to the applied bias, in agreement with our calculations. Therefore, the electric-field difference cannot account for an energy shift of the $e1$-$e3$ transition. Instead, transition $e1$-$e3$ in the absorption spectrum is obscured by a broad shoulder which originates from $e1$ transitions into the Γ continuum of the $Ga_{0.6}Al_{0.4}As$ barrier. The fact that the $e1$-$e3$ transition dominates the photocurrent spectrum is explained as follows. State $e3$ is loosely bound and with an electric field it is "pushed" into the continuum. Therefore, only electrons excited to $e3$ can propagate toward the positive electrode without tunneling hinderance. Similar elimination of tunneling in a FBSQW detector produces high-D^* detectors.[7] Our result, therefore, suggests that when using an asymmetrical structure, it is possible to achieve high D^* 5-μm detectors with $GaAs/Ga_{1-x}Al_xAs$ MQW. The origin of the broad transition marked x is not clear to us. Transitions a, b, and c are unique to this structure and can be explained with the model described below.

We have used Airy functions in the transfer-matrix technique to calculate the wave functions and energy states of the structure[17] under electric field. In the calculations we used an energy-dependent effective mass to account for the nonparabolic effective mass in the QW's:

$$m^*_{QW} = (0.0665 + 0.0436E + 0.236E^2 - 0.147E^3)m_0 ,$$

where m_0 and m^*_{QW} are the free-electron mass and the energy-dependent effective mass in the QW,[20] respectively. The electron energy E here is measured from the bottom of a particular QW and not from a fixed point of reference of the structure. The electron effective mass in the barrier is given by:[21,22] $m^*_b = (0.0665 + 0.083x)m_0$, where x is the barrier Al content. We have used a conduction-band offset of $\Delta E_c = 323$ meV for $x = 0.4$.[2] In order to take screening into account, we used a layer dependent electric field such that the bias potential is dropped equally across all layers except for the doped layer, where the field is minimal. Using this approach, we calculated states confined to a 19-layer structure as shown in Fig. 3, i.e., we required the decay of the electron wave function to the left and to the right of this structure as boundary conditions, and we ignored the periodicity of the test structure. The calculated energies as a function of the

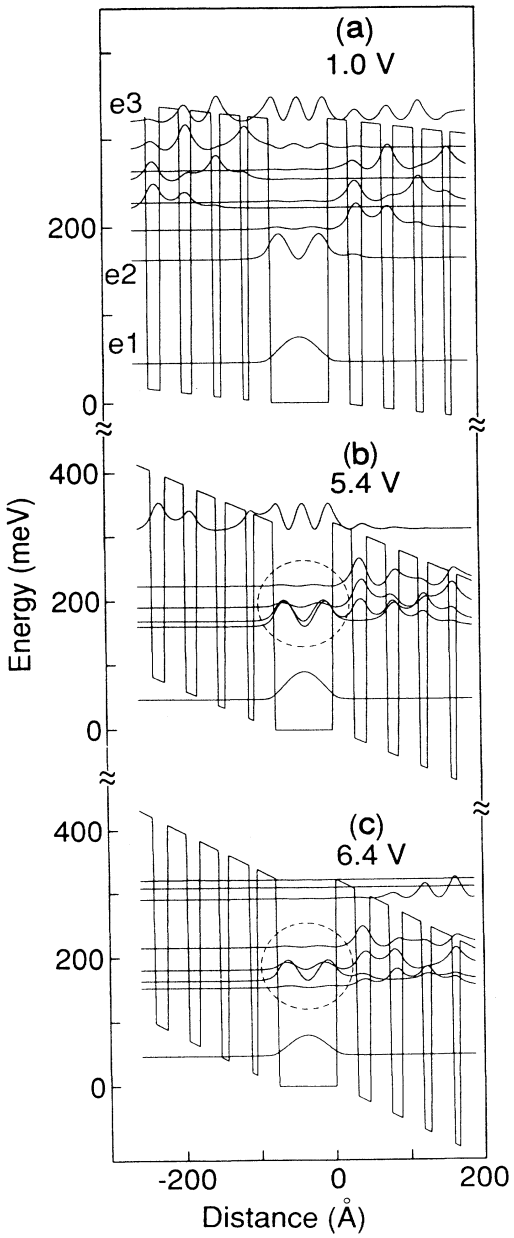

FIG. 3. Band diagram of a section of the MQW structure, and its squared wave functions as calculated for 3 different bias voltages.

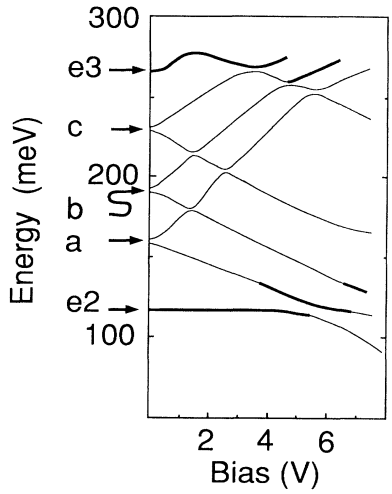

FIG. 4. The dependence of the calculated confined states on the electric field expressed as the bias voltage across the device. Energy is measured relative to the ground state $e1$. States with significant dipole moment with the ground state are marked with thick lines.

bias voltage (applied across a 30 period structure) is presented in Fig. 4. In the calculation, we find three states that are localized to the thick QW: the ground state of the system $e1$, and two excited states, $e2$ and $e3$. We also find three pairs of subband states, marked at zero bias as a, b, and c. The wave functions of the states which comprise these pairs, in the $0.1 < V < 2$ bias range, are localized either to the left or to the right VSSEF, as depicted in Fig. 3(a). However, at zero bias the wave function of the left state overlaps the state on the right of the same pair, and due to the degeneracy of the left and right VSSEF energies, they split to form a two-state "band". In the test structure there are 30 periods and therefore it should give rise to a 30-state band. Despite the simplicity of the model, it explains the experimental data without adjustable parameters. When compared to the absorption data, the calculated energy difference from the ground state $e1$ to states a, b, c, $e2$, and $e3$ produce an excellent fit to the observed values, as is summarized in Table I.

In order to examine the electronic energy filtering properties of the VSSEF structure in the framework of our model, we performed the following experiment. We measured the photocurrent response as a function of the detector bias voltage while exposed to a 1 mW, 9.5-μm CO_2 laser. Such monochromatic illumination assures selective excitation of state $e2$ up to the crossing voltage, and of the next excited state after crossing (Fig. 4). The results depicted in Fig. 5 show a distinct resonance at 5.7 V followed by a negative differential conductance. The response persists from 10 to 90 K where it smears out. This photoinduced resonant tunneling effect stems from the crossing of the first excited state $e2$ with the second (Fig. 4), calculated to occur at $\sim$5.4 V, and is explained as follows. The photocurrent signal may be viewed as propor-

TABLE I. Calculated (Fig. 4) and observed (Fig. 2) LWIR transition energies.

Transition	$e1$-$e2$	a	b	c	$e1$-$e3$	x
Observed absorption energy (meV)	124	164	195	225	250–310	427
Observed photocurrent energy (meV)	...	...	...	...	250	...
Calculated energy (meV)	117	160	195	232	268	...

tional to the electron photoexcitation probability (oscillator strength) from $e1$ to $e2$ and to the probability of an electron to tunnel from $e2$ to the continuum. In Figs. 3(b) and 3(c), we encircled the wave functions of the involved states at and after the resonance. At low bias, before resonance [see Fig. 3(a)], the interaction between the excited electron in $e2$ which is completely localized to the thick QW, and the next excited state which has a substantial component in the continuum is small. Therefore, a small photocurrent is expected. At the resonance [see Fig. 3(b)], where the states cross, the mixing becomes large and both have high oscillator strengths for transitions from the ground state, associated with high tunneling probability with the continuum, and therefore a high photocurrent signal is achieved. After resonance [see Fig. 3(c)], $e2$ becomes a tunneling state but has diminished oscillator strength, whereas the next excited state has high oscillator strength for transition from $e1$, but also has low tunneling probability, and therefore the photocurrent signal is small again. This result is the first direct observation of photon assisted resonant tunneling, and it shows that electrons can be filtered to create a monochromatic beam. A LWIR laser may be possible once two such filters can be made to work simultaneously, one to inject selectively into an excited state and one, as in the present structure, to pump electrons out of the laser's ground state, to create population inversion.[16]

In conclusion, we have tested and analyzed an asymmetrically structured MQW structure and find that GaAs/$Ga_{1-x}Al_xAs$ can be used for LWIR detectors to cover the 3–6-μm atmospheric window. Better design is necessary in order to suppress the dark current. The properties of the structure were explained by calculating the energy states of the structure under bias, using the transfer-matrix technique, with excellent agreement. We also discussed the electronic filtering capability of the structure, manifested by the observation of photon assisted resonant tunneling at 10 μm.

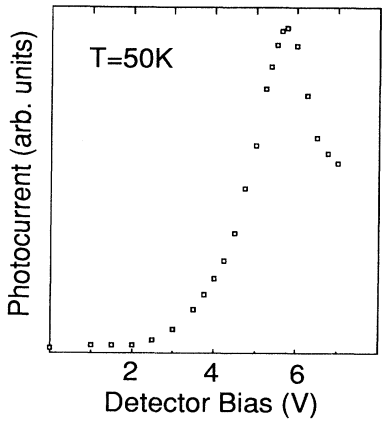

FIG. 5. Photocurrent response of the device with 9.5-μm CO_2 laser illumination which shows a peak and negative differential conductance of the photon assisted resonant tunneling.

S.I.B. thanks Dr. Amos Ori for useful discussions. Some of the research described here was sponsored by the Strategic Defense Initiative Organization, Innovative Science and Technology Office and the National Aeronautics and Space Administration. The research at Chalmers University was sponsored by the Swedish Board for Technical Development.

[1]B. F. Levine, R. J. Malik, J. Walker, K. K. Choi, C. G. Bethea, D. A. Kleinman, and J. M. Vandenberg, Appl. Phys. Lett. **50**, 273 (1987).

[2]N. Nakayama, H. Kuwahara, H. Kato, and K. Kubota, Appl. Phys. Lett. **51**, 1741 (1987).

[3]K. K. Choi, B. F. Levine, C. G. Bethea, J. Walker, and R. J. Malik, Phys. Rev. Lett. **59**, 2459 (1987).

[4]B. F. Levine, A. Y. Cho, J. Walker, R. J. Malik, D. A. Kleinman, and D. L. Sivco, Appl. Phys. Lett. **52**, 1481 (1988).

[5]W. Cai, T. F. Zheng, P. Hu, M. Lax, K. Shum, and R. R. Alfano, Phys. Rev. Lett. **65**, 104 (1990).

[6]B. C. Covington, C. C. Lee, B. H. Hu, H. F. Tailor, and D. C. Streit, Appl. Phys. Lett. **54**, 2145 (1989).

[7]B. F. Levine, G. Hasnain, C. G. Bethea, and N. Chand, Appl. Phys. Lett. **54**, 2704 (1989).

[8]M. M. Fejer, S. J. B. Yoo, R. L. Byer, A. Harwit, and J. S. Harris, Jr., Phys. Rev. Lett. **62**, 1041 (1989).

[9]P. F. Yuh and K. L. Wang, Appl. Phys. Lett. **51**, 1404 (1987).

[10]M. Helm, P. England, E. Colas, F. DeRosa, and S. J. Allen, Jr., Phys. Rev. Lett. **63**, 74 (1989).

[11]S. I. Borenstain and J. Katz, Appl. Phys. Lett. **55**, 654 (1989).

[12]Y. J. Mii, R. P. G. Karunasiri, K. L. Wang, M. Chen, and P. F. Yuh, Appl. Phys. Lett. **56**, 1986 (1990).

[13]J. L. Pan, L. C. West, S. J. Walker, R. J. Malik, and J. F. Walker, Appl. Phys. Lett. **57**, 1366 (1990).

[14]B. F. Levine, C. G. Bethea, V. O. Shen, and R. J. Malik, Appl. Phys. Lett. **57**, 383 (1990).

[15]K. F. Brennan and C. J. Summars, J. Appl. Phys. **61**, 614 (1987).

[16]S. I. Borenstain and J. Katz, Phys. Rev. B **39**, 10852 (1989).

[17]D. Campi and C. Alibert, Appl. Phys. Lett. **55**, 454 (1989); D. C. Hutchings, Appl. Phys. Lett. **55**, 1082 (1989).

[18]L. C. West and S. J. Eglash, Appl. Phys. Lett. **46**, 1156 (1985).

[19]A. Harwit and J. S. Harris, Jr., Appl. Phys. Lett. **50**, 685 (1987).

[20]Z. Y. Xu, V. G. Kreismanis, and C. L. Tang, Appl. Phys. Lett. **43**, 415 (1983).

[21]H. C. Casey, Jr. and M. B. Panish, *Heterostructure Lasers* (Academic, New York, 1978), Pt. A, p. 192.

[22]We note that for a symmetrically structured GaAs/AlAs superlattice, the effective mass in the barrier has been treated more rigorously using a four-band $\mathbf{k}\cdot\mathbf{P}$ model [see G. Brozak, E. A. de Andrada e Silva, L. J. Sham, F. DeRosa, P. Miceli, S. A. Schwarz, J. P. Harbison, L. T. Florez, and S. J. Allen, Jr., Phys. Rev. Lett. **64**, 471 (1990)]. The barrier effective mass formula used in our calculation (Ref. 21), combined with the GaAs energy-dependent mass (Ref. 20), takes into account many body effects and other effects due to the energy dependence of the barrier effective masses. We choose this phenomenological approach because its simplicity facilitates an Airy-function-based solution for the wave functions in our asymmetrical structure.